

## From Salts to Ionic Liquids by Systematic Structural Modifications: A Rational Approach Towards the Efficient Modular Synthesis of Enantiopure Imidazolium Salts

Nicolás Ríos-Lombardía,<sup>[a]</sup> Eduardo Busto,<sup>[a]</sup> Vicente Gotor-Fernández,<sup>[a]</sup>  
Vicente Gotor,<sup>\*,[a]</sup> Raúl Porcar,<sup>[b]</sup> Eduardo García-Verdugo,<sup>[b, f]</sup> Santiago V. Luis,<sup>\*,[b]</sup>  
Ignacio Alfonso,<sup>[c]</sup> Santiago García-Granda,<sup>[d]</sup> and Amador Menéndez-Velázquez<sup>[e]</sup>

**Abstract:** This paper reports a simple and robust modular synthetic strategy that leads to a large variety of configurationally and structurally diverse imidazole-based chiral ionic liquids (CILs) by lipase-catalyzed resolution. The intimate microscopic interactions of the supramolecular ionic network of these imidazolium chiral salts at the molecular level are investigated both spectroscopically (NMR, FT-IR-ATR) and theoretically, and a topological analysis of the experimental electron densities obtained by X-ray diffraction of single crystals is performed. Our results support the key role played by the relative configuration of the -OR group on the hydrogen-bonding pattern and its

strong influence on the final physical properties of the imidazolium salt. We also obtained a reasonable correlation between the observed melting point and the non-covalent interactions. The spectroscopic data and the topological analysis reflect the key role played by hydrogen bonds between the OH and imidazolium C2H groups in both cation-anion and cation-cation interactions, with the presence of an OH group leading to an additional interaction interaction. This interaction sig-

**Keywords:** chirality · green chemistry · imidazolium salts · ionic liquids · lipases

nificantly affects the properties of stereoisomeric salts. Even more interestingly, we also studied the effect of the chirality by comparing enantiopure CILs with their racemic mixtures and found that, with the exception of *trans*-Cy6-OH-Im-Bn-Br, the melting points of the racemic mixtures are higher than those of the corresponding enantiomerically pure forms. For stereoisomeric examples, we have successfully explained the differences in melting temperatures in light of the corresponding structural data. Chirality should therefore be taken into account as a highly attractive design vector in the preparation of ILs with specifically desired properties.

[a] N. Ríos-Lombardía, Dr. E. Busto, Dr. V. Gotor-Fernández, Prof. V. Gotor  
Departamento de Química Orgánica e Inorgánica  
Instituto Universitario de Biotecnología de Asturias  
Universidad de Oviedo, 33071 Oviedo (Spain)  
Fax: (+34)985103448  
E-mail: vgs@fq.uniovi.es

[b] R. Porcar, Dr. E. García-Verdugo, Prof. S. V. Luis  
Departamento de Química Inorgánica y Orgánica  
Universitat Jaume I, 12071 Castellón de la Plana (Spain)  
Fax: (+34)964-728-214  
E-mail: luiss@qio.uji.es

[c] Dr. I. Alfonso  
Departamento de Química Biológica y Modelización Molecular  
Instituto de Química Avanzada de Cataluña (IQAC)  
Consejo Superior de Investigaciones Científicas (CSIC)  
Jordi Girona 18-26, 08034 Barcelona (Spain).

[d] Prof. S. García-Granda  
Departamento de Química Física y Analítica  
Universidad de Oviedo, 33071 (Spain)

[e] Dr. A. Menéndez-Velázquez  
Centro de Investigación en Nanomateriales y Nanotecnología (CINN)  
Instituto Tecnológico de Materiales de Asturias (ITMA)  
Parque Tecnológico de Asturias, 33428 Llanera (Spain)

[f] Dr. E. García-Verdugo  
Instituto de Catálisis y Petroleoquímica, CSIC, Campus de la UAM  
C/ Marie Curie, 2; Cantoblanco; Madrid; 28049 (Spain)

 Supporting information for this article is available on the WWW under <http://dx.doi.org/10.1002/chem.200901623> and includes general experimental procedures, a full list of the ionic liquids prepared, with their isolated yields and melting points, DFT calculations, the thermal stability study by TGA, and the topological analysis of the experimental electron densities.

## Introduction

Inorganic salts, such as NaCl, usually melt at very high temperatures. However, many salts with organic cations and/or anions can be found in their liquid state at moderate temperatures. This fact has led to their routine use as solvents for chemical processing, whereupon they are referred to as “ionic liquids” (ILs). This term describes organic salts that are liquid at or near room temperature, with 100 °C as an arbitrary upper limit.<sup>[1]</sup> ILs seem to be ideal replacement solvents since they exhibit low vapor pressures and high boiling points due to their very strong ion–ion interactions. ILs are currently attracting considerable attention as reaction solvents,<sup>[2,3]</sup> extraction liquids,<sup>[4]</sup> and electrolyte materials<sup>[5]</sup> as a result of their remarkable properties.

The physicochemical characteristics of ILs depend on the interaction established between both the cation and the anion.<sup>[6]</sup> Thus, the large potential structural diversity of ILs plays an important role in our ability to define their final properties.<sup>[7]</sup> Indeed, ILs are now expected to be tailor-made with controllable physical and chemical properties or even specific functions (task-specific ionic liquids, TSILs).<sup>[8]</sup>

Among the many different design vectors, chirality can be considered by far the most interesting for organic chemists. Indeed, a great deal of effort has been expended in the last few years to design and synthesize chiral ionic liquids (CILs).<sup>[9]</sup> However, most of the currently known CILs have a major structural limitation: they are relatively restricted in terms of chiral structural diversity as they are derived from the chiral pool.<sup>[10,11]</sup> Different studies have established the influence of side chains as well as the presence of additional functional groups on the intrinsic physical properties of ILs.<sup>[1,12]</sup> However, although some studies have attempted to correlate the configurational properties of chiral compounds with their corresponding macroscopic behavior,<sup>[13]</sup> as far as we are aware there is no systematic study within the field of CILs. Such a study would require an in-depth knowledge of the intimate microscopic interactions at the molecular level.

Herein we report a simple and robust modular synthetic strategy that leads to a large variety of configurationally and structurally diverse CILs. This approach allows us to reach a bottom-up understanding of the structure–property relationship based on the study of these CILs. NMR and ATR-FT-IR analyses, theoretical calculations, and topological analysis of experimental electron densities reveal the significant influence of chirality on the final structure and properties of ILs. In light of these data, the relationships between the relative and absolute configurations of the chiral stereocenters of different chiral imidazolium salts and one of their key physical macroscopic properties, namely the melting point ( $T_m$ ), have been established for the first time. Our results highlight the importance of the configuration of chiral centers as new design vectors when preparing ionic liquid with desired macroscopic properties.

## Results and Discussion

**Molecular design and chemoenzymatic synthesis:** A simple synthetic strategy has been designed for the preparation of chiral imidazolium salts. Figure 1 summarizes the five tun-

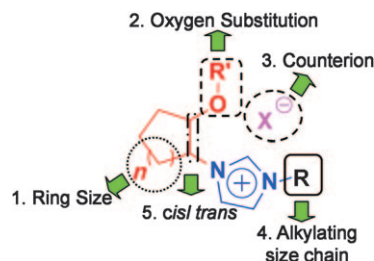
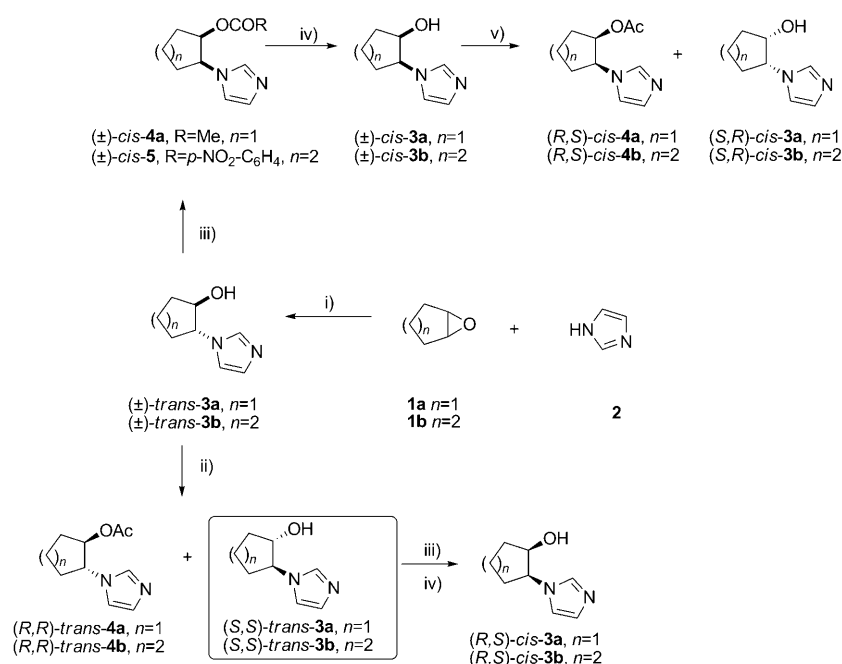


Figure 1. Design vectors employed in the synthesis of chiral imidazolium salts.

able molecular engineering vectors selected as the design variables: 1) the ring size (five- or six-membered ring); 2) oxygen substitution ( $R' = \text{H}$  or  $\text{Ac}$ ); 3) the nature of the counterion ( $X^- = \text{Cl}^-$ ,  $\text{Br}^-$ ,  $\text{BF}_4^-$ , or  $\text{NTf}_2^-$ ); 4) the imidazole alkylating side-chain ( $R = \text{Bn}$ ,  $n\text{Bu}$ , or  $n\text{Oct}$ ); 5) the configuration at the two stereogenic centers and, in particular, the relative disposition (*cis* or *trans*) of the imidazole and OR groups on the cycloalkane ring. These modifications lead to different stereoisomeric chiral imidazolium salts. The three first variables have been used previously to prepare room-temperature ionic liquids (RTILs), therefore their influence on the macroscopic properties of RTILs is beginning to be understood.<sup>[1,12,14]</sup> However, geometric modifications such as ring size or the configuration around the chiral centers have not been studied previously in a systematic manner.

Scheme 1 summarizes the synthetic strategy followed to prepare enantiopure imidazoles derived from ( $\pm$ )-*trans*-2-(1*H*-imidazol-1-yl)cyclopentanol [( $\pm$ )-*trans*-**3a**] and ( $\pm$ )-*trans*-2-(1*H*-imidazol-1-yl)cyclohexanol [( $\pm$ )-*trans*-**3b**]. The racemic alcohols (**3a–b**) were prepared in good yields by treating the corresponding cyclic epoxides **1a–b** with imidazole (**2**), following the procedure previously described by Yus and co-workers.<sup>[15]</sup> They were then enzymatically resolved to yield the enantiopure acetates (*R,R*)-*trans*-**4a** and **-4b** and the alcohols (*S,S*)-*trans*-**3a** and **-3b** under mild reaction conditions by using *Candida antarctica* lipase type B (CAL-B) or different *Pseudomonas cepacia* lipase preparations immobilized on ceramics (PSL-C I or PSL-C II). The optimization process is summarized in Table 1. All biocatalysts tested showed an excellent stereoselectivity towards the formation of (*R,R*)-*trans* acetates **4a–b** and (*S,S*)-*trans* alcohols **3a–b**, which were isolated in enantiopure form with very high yields (entries 2 and 7, Table 1).<sup>[16]</sup> The absolute stereochemistries of alcohols (*S,S*)-*trans*-**3a–b** and acetylated derivatives (*R,R*)-*trans*-**4a–b** were assigned after X-ray analysis of the alcohol recovered from the enzymatic kinetic resolution of racemic ( $\pm$ )-*trans*-**3a**, which showed a clear preference of the enzyme to acetylate the 1-(*R*) position.<sup>[17]</sup>



Scheme 1. Chemoenzymatic stereoselective synthesis of enantiopure *cis*- and *trans*-2-(1*H*-imidazol-1-yl)cyclopentanol and -cyclohexanol derivatives: i) ref. 14; ii) kinetic resolution, enzyme, vinyl acetate, solvent (see Table 1); iii) RCOOH (R=Me for **3a** and R=*p*-NO<sub>2</sub>-C<sub>6</sub>H<sub>4</sub> for **3b**), DEAD, PPh<sub>3</sub>, THF; iv) K<sub>2</sub>CO<sub>3</sub>, MeOH, H<sub>2</sub>O; v) kinetic resolution, enzyme, vinyl acetate, solvent (see Table 2).

Table 1. Enzymatic kinetic resolution of alcohols (±)-*trans*-**3a–b** using vinyl acetate as acyl donor.

Entry	Substrate	Enzyme	<i>T</i> [°C]	<i>ee</i> <sub>S</sub> [%] <sup>[a]</sup>	<i>ee</i> <sub>P</sub> [%] <sup>[a]</sup>	<i>c</i> [%] <sup>[b]</sup>	<i>E</i> <sup>[c]</sup>
1	(±)- <i>trans</i> - <b>3a</b>	CAL-B <sup>[d]</sup>	30	99 (92)	>99 (91)	50	>200
2	(±)- <i>trans</i> - <b>3a</b>	PSL-C I <sup>[d]</sup>	30	>99 (92)	>99 (94)	50	>200
3	(±)- <i>trans</i> - <b>3a</b>	PSL-C II <sup>[d]</sup>	30	97 (88)	>99 (91)	49	>200
4	(±)- <i>trans</i> - <b>3b</b>	CAL-B <sup>[d]</sup>	30	93 (87)	98 (85)	49	>200
5	(±)- <i>trans</i> - <b>3b</b>	PSL-C II <sup>[d]</sup>	30	97 (90)	98 (88)	50	>200
6	(±)- <i>trans</i> - <b>3b</b>	PSL-C II <sup>[e]</sup>	30	33 (96)	>99 (90)	25	>200
7	(±)- <i>trans</i> - <b>3b</b>	PSL-C II <sup>[e]</sup>	45	>99 (93)	>99 (91)	50	>200

[a] Determined by HPLC; yields in brackets refer to the corresponding conversion value. [b]  $c = ee_S / (ee_S + ee_P)$  in which the subscripts S and P stand for substrate and product, respectively. [c]  $E = \ln[(1-c) \times (1-ee_S)] / \ln[(1-c) \times (1+ee_S)]$ .<sup>[18]</sup> [d] THF as solvent. [e] *tert*-Butyl methyl ether (TBME) as solvent.

Synthesis of the *cis* derivatives was also attempted in order to get *cis/trans* structural modularity. Thus, the (±)-*cis*-alcohols were easily prepared from the corresponding *trans* derivatives by means of a Mitsunobu inversion. Acetic acid was used for (±)-*trans*-**3a** whereas *p*-nitrobenzoic acid was used for (±)-*trans*-**3b** due to the poor reactivity observed with AcOH. The (±)-*cis* esters **4a** and **5** were deprotected with potassium carbonate to give the racemic alcohols (±)-*cis*-**3a** and **3b** in high overall yields. The inversion of configuration was clearly observed upon comparing the <sup>1</sup>H NMR spectra for (±)-*cis* and (±)

*trans* alcohols, especially for the cyclohexanol derivatives.<sup>[17]</sup>

Enzymatic kinetic resolution was then carried out to prepare the corresponding enantiopure *cis* compounds. Both (±)-*cis*-**3a** and **3b** were treated with three equivalents of vinyl acetate as acyl donor and different enzymes as catalysts (see Table 2). As expected, the *cis* compounds were less reactive than the *trans*-derivatives in lipase-catalyzed reactions, especially in the case of the six-membered cycles.<sup>[18]</sup> Cyclopentanol (±)-*cis*-**3a** showed an excellent enantioselectivity towards formation of the acetate (*R,S*)-**4a**, although a lower reaction rate was observed in comparison with the corresponding *trans* derivative. This meant that higher temperatures were needed to reach 50% conversion. Both the acetate and the alcohol were isolated with 94% *ee* (entry 2, Table 2). Alternatively, PSL-C II catalyzed the acetylation of (±)-*cis*-**3a** to give the enantioenriched products in almost enantiopure form and with very high isolated yields (entry 3, Table 2). The absolute stereochemistries of enantiopure alcohol *cis*-(*S,R*)-**3a** and acetate *cis*-(*R,S*)-**4a** were assigned by X-ray analysis of the crystallized compounds after

the enzymatic process.<sup>[17]</sup>

The enzymatic kinetic resolution of (±)-*cis*-**3b** was also conducted with CAL-B and PSL-C II (entries 4 and 5, Table 2), although the results were rather disappointing as

Table 2. Enzymatic kinetic resolution of alcohols (±)-*cis*-**3a–b** using three equivalents of vinyl acetate in dry THF at 250 rpm.

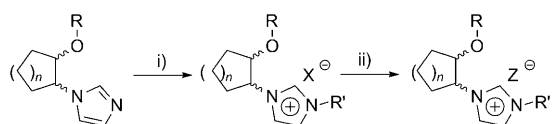
Entry	Substrate	Enzyme	<i>T</i> [°C]	<i>t</i> [h]	<i>ee</i> <sub>S</sub> [%] <sup>[a]</sup>	<i>ee</i> <sub>P</sub> [%] <sup>[a]</sup>	<i>c</i> [%] <sup>[b]</sup>	<i>E</i> <sup>[c]</sup>
1	<i>cis</i> - <b>3a</b>	CAL-B	30	161	44 (81)	>99 (83)	31	>200
2	<i>cis</i> - <b>3a</b>	CAL-B	60	63	94 (87)	94 (76)	50	115
3	<i>cis</i> - <b>3a</b>	PSL-C II	60	23	96 (96)	99 (93)	49	>200
4	<i>cis</i> - <b>3b</b>	CAL-B	60	53.5	–	–	50	–
5	<i>cis</i> - <b>3b</b>	PSL-C II	60	25	54	54	50	6
6	<i>cis</i> - <b>3b</b>	CRL	60	72	–	–	50	–
7	<i>cis</i> - <b>3b</b>	PPL	60	72	4	9	31	1
8	<i>cis</i> - <b>3b</b>	CAL-A	60	72	10	58	15	4

[a] Determined by HPLC and isolated yields in brackets referred to the corresponding conversion value. [b]  $c = ee_S / (ee_S + ee_P)$ . [c]  $E = \ln[(1-c) \times (1-ee_S)] / \ln[(1-c) \times (1+ee_S)]$ .<sup>[18]</sup>

no or only poor enantioselectivity for acylation of the racemic alcohol was achieved. Similarly low activities and enantioselectivities were observed with other biocatalysts [*Candida rugosa* lipase (CRL), Porcine pancreas lipase (PPL) or *Candida antarctica* lipase type A (CAL-A)] (entries 6–8, Table 2).

In light of these results, a different synthetic strategy starting from the enantiopure alcohols (*S,S*)-*trans*-**3a** and **-3b**, previously prepared by enzymatic kinetic resolution, and involving Mitsunobu inversion and deprotection steps was evaluated. This synthetic methodology led to enantiopure alcohols (*R,S*)-*cis*-**3a** and (*R,S*)-*cis*-**3b** with 78% and 85% isolated yields, respectively.

Finally, the preparation of optically active imidazolium salts was performed from either the *cis/trans* acetates or alcohols by treatment with the corresponding alkyl or aryl halide (Scheme 2). Exchange of the halide present in the ini-



Scheme 2. Schematic representation of the synthesis of chiral 2-(1*H*-imidazol-1-yl)cyclopentanol and -cyclohexanol salts from enantiopure compounds prepared according to Scheme 1: i) R'X, 70 or 100 °C; ii) NaBF<sub>4</sub> or LiNTf<sub>2</sub>, MeOH/H<sub>2</sub>O, room temperature.

tial imidazolium salts with different anions (BF<sub>4</sub><sup>-</sup> or NTf<sub>2</sub><sup>-</sup>) occurred with very high yields to give a family of more than 30 enantiopure chiral imidazolium salts with significant structural diversity.<sup>[16,19]</sup> Since some of the obtained salts are hygroscopic, they were carefully dried in an oven at high vacuum before characterization.

### Phase transition (melting points) for the chiral imidazolium salts:

The phase transitions (melting points, *T*<sub>m</sub>) of the newly synthesized CILs were measured in order to compare their physical properties. Thus, a dried sample of the corresponding salt was placed in an open DSC pan and heated at 130 °C for 120 min. Three complete cycles of heating and cooling at a rate of 5 °C/min were then performed to clearly identify the corresponding phase transitions. All these operations were carried out under nitrogen. Table 3 illustrates some of the solid–liquid phase transitions for the newly prepared imidazolium salts, as measured by differential scanning calorimetry (DSC) in the temperature range –50 to

Table 3. Effect of the alkyl chain (Bn, Bu, or Oct) and counteranion (Br<sup>-</sup>, Cl<sup>-</sup>, BF<sub>4</sub><sup>-</sup>, or NTf<sub>2</sub><sup>-</sup>) on the melting points (*T*<sub>m</sub>) for some *trans* chiral imidazolium salts.

	<i>(S,S)</i> - <i>trans</i> -Cy5-OH-[a]				<i>(S,S)</i> - <i>trans</i> -Cy6-OH-[a]			
	Br <sup>-</sup>	Cl <sup>-</sup>	BF <sub>4</sub> <sup>-</sup>	NTf <sub>2</sub> <sup>-</sup>	Br <sup>-</sup>	Cl <sup>-</sup>	BF <sub>4</sub> <sup>-</sup>	NTf <sub>2</sub> <sup>-</sup>
-Bn-	112	–	–9	–42	188	219	6	–29
-Bu-	–	–21	–47	<–50	–	7	–22	–50
-Oct-	–	–30	–48	<–50	–	2	–35	–51

[a] Melting temperatures [°C] for a heating rate of 10 °C min<sup>-1</sup> calculated at onset.

400 °C.<sup>[20]</sup> The *T*<sub>m</sub> is an important parameter because it can be related to other properties of ionic liquids, such as viscosity or conductivity.<sup>[1]</sup>

In general, cyclopentanol-derived imidazolium salts were found to have lower melting points than those derived from cyclohexanol. As expected, the introduction of nonbasic, noncoordinating anions such as BF<sub>4</sub><sup>-</sup>, or organic amides such as NTf<sub>2</sub><sup>-</sup>, into the chiral salts led to lower melting points than with halide anions (Br<sup>-</sup> or Cl<sup>-</sup>) as counterions.<sup>[1]</sup> The tendency towards the formation of solid ionic salts for different anions decreases in the order Cl<sup>-</sup> > Br<sup>-</sup> > BF<sub>4</sub><sup>-</sup> > NTf<sub>2</sub><sup>-</sup>. Indeed, organic salts containing BF<sub>4</sub><sup>-</sup> or NTf<sub>2</sub><sup>-</sup> can be considered to be chiral RTILs for all the cases studied (*T*<sub>m</sub> < 100 °C). The size and nature of the alkylating agent (Step *i* in Scheme 2) also play a key role in determining the melting point of the different enantiopure chiral imidazolium salts, with the general trend observed for the melting temperatures being as follows: Bn > *n*Bu > *n*Oct. As a matter of fact, the chiral salts obtained upon alkylation with benzyl bromide and benzyl chloride showed high melting points and were easily obtained as crystalline materials, in some cases forming crystals appropriate for subsequent crystallographic analysis (see below).

More interesting, however, were the results observed for the series of compounds shown in Figure 2. For this family

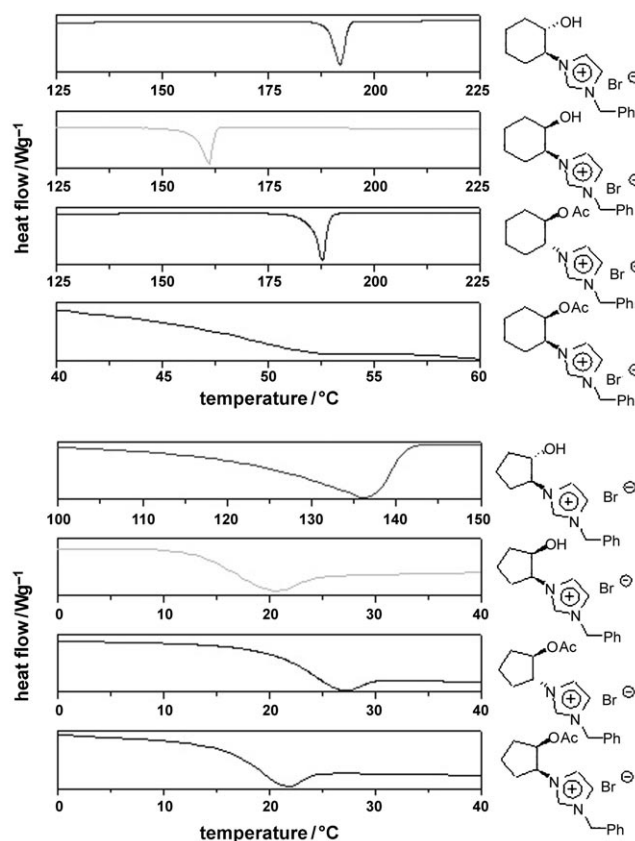


Figure 2. DSC plots for a family of enantiopure chiral imidazolium salts with controlled structural modifications [*T*<sub>m</sub> (°C) calculated at onset; heating rate: 5 °C min<sup>-1</sup>]. The curves correspond to the third DSC cycle of melting.

of compounds, controlled structural modifications in ring size, oxygen substitution, and *cis/trans* geometry were systematically introduced whilst keeping the bromide anion and the benzyl group as common structural elements. The corresponding melting temperatures and DSC traces are shown in Figure 2.

The first conclusion that can be derived from Figure 2 is that salts containing five-membered rings have lower melting points than those bearing six-membered rings (left side in Figure 2), as previously observed for other series of salts. Furthermore, the structural modifications have a more significant impact in the C5 derivatives than in the C6 ones. The nature of the OR groups also seems to play an important role in determining the final macroscopic properties of the chiral salt. Indeed, the melting point varies significantly from the alcohols to the corresponding acetylated derivatives. Finally, it can also be seen that for the isomeric molecular chiral salts, the *cis* derivatives lead to lower melting points than the corresponding *trans* isomers.

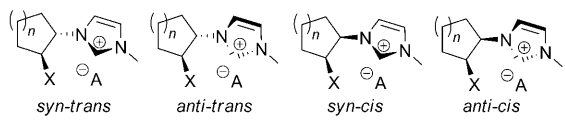
The thermal stability of the ionic liquids was also assessed by thermogravimetric analysis. In general, the TGA plots for the different NTf<sub>2</sub> derivatives show the high stability of the compounds up to 200 °C (see Supporting Information). For example, when (*S,S*)-*trans*-Cy6-OH-Im-Bn-NTf<sub>2</sub> was heated at 150 °C for a period of three hours, the compound did not show any signals of decomposition upon <sup>1</sup>H NMR spectroscopic analysis after cooling. We can therefore conclude that the disposition and geometry of both OH/OR groups and the imidazolium ring are very important for determining the macroscopic properties of the imidazolium salts. The former data suggest that interactions between OH and C2-H are likely to play a key role in determining the structural properties of the CILs. This is also highlighted by the fact that the bromide salts of cyclopentylbenzyl imidazolium (Cy5-Im-Bn-Br) and cyclohexylbenzyl imidazolium (Cy6-Im-Bn-Br) are liquids at room temperature.

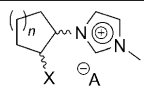
**Theoretical and spectroscopic studies:** We performed theoretical quantum mechanics calculations in order to try to understand the differences in physical properties observed for the CILs. DFT calculations at the B3LYP/6-31+G\* level of theory were performed on isolated ionic pairs of model systems bearing a methyl group at N3 of the imidazolium ring.<sup>[21]</sup> Since we suspected that the physical properties could be related to the inter-ion contacts, the anion–cation interaction energy ( $E_{\text{int}}$ ) was computed using the following [Eqn (1)]:

$$E_{\text{int}} = E(\text{isolated ionic pair}) - [E(\text{isolated cation}) + E(\text{isolated anion})] \quad (1)$$

Some results from the theoretical analysis are shown in Table 4. As regards the effect of the anion, the interaction energy decreases in the series Cl<sup>-</sup> > Br<sup>-</sup> > BF<sub>4</sub><sup>-</sup> (Table 4, entries 5, 7 and 8), as expected on the basis of previously reported ILs and in accordance with the melting temperatures measured for our compounds.<sup>[6]</sup>

Table 4. Interaction energies for the computed (B3LYP/6-31+G\*) model ionic liquids.



Entry		$-E_{\text{int}}(\text{syn})^{[a]}$ [kcal mol <sup>-1</sup> ]	$-E_{\text{int}}(\text{anti})^{[a]}$ [kcal mol <sup>-1</sup> ]
1	( <i>R,S</i> )- <i>cis</i> -Cy5-OH-Im-Me-Br	88.23	88.05
2	( <i>S,S</i> )- <i>trans</i> -Cy5-OH-Im-Me-Br	87.32	88.85
3	( <i>S,S</i> )- <i>trans</i> -Cy5-OAc-Im-Me-Br	83.39	84.55
4	( <i>R,S</i> )- <i>cis</i> -Cy6-OH-Im-Me-Br	87.86	86.09
5	( <i>S,S</i> )- <i>trans</i> -Cy6-OH-Im-Me-Br	88.40	89.06
6	( <i>R,R</i> )- <i>trans</i> -Cy6-OAc-Im-Me-Br	83.39	79.81
7	( <i>S,S</i> )- <i>trans</i> -Cy6-OH-Im-Me-Cl	93.78	93.87
8	( <i>S,S</i> )- <i>trans</i> -Cy6-OH-Im-Me-BF <sub>4</sub>	85.01	84.80
9	Cy6-Im-Me-Br	82.89	–

[a] The *syn/anti* conformations refer to the relative disposition between X and the imidazolium C2-H group (see the Supporting Information for details).

Our theoretical calculations also reflected a stabilization effect of the OH group. Thus, elimination of the OH group in the cyclohexane derivative weakens the anion–cation interaction with bromide by around 6.2 kcal mol<sup>-1</sup> (Table 4, entries 5 and 9). Moreover, acetylation of the OH group also decreases the interaction energy by 5.7 kcal mol<sup>-1</sup> (Table 4, entries 5 and 6). Both experimental data and calculations strongly support the stabilization effect of the OH...anion hydrogen-bonding interactions, although secondary inter-cationic interactions (such as additional H bonding, π–π or C-H...π bonding involving benzyl aromatic rings), which were not considered in the calculations but were observed in the crystal structures (see X-ray section below), could also contribute significantly to the global stability of the salts. The presence of additional functionalities in the ILs, which are able to form hydrogen-bond interactions with the counterion, has a significant influence on their final macroscopic properties<sup>[12,22]</sup>

As regards the conformation of the chiral cations, the imidazolium group is located in one equatorial position of the cycle in all cases. The cyclohexane derivatives have perfect chair-like conformations, thus placing the OH group equatorial for the *trans* isomers and axial for *cis* isomers. The cyclopentane rings display an envelope conformation. The imidazolium ring can have the C2-H moiety in two different positions: *syn* [for (*R,R*)-*trans*-Cy6-OAc-Im-Me-Br and for (*R,S*)-*cis*-Cy6-OH-Im-Me-Br] or *anti* [for (*S,S*)-*trans*-Cy6-OH-Im-Me-Cl, (*S,S*)-*trans*-Cy5-OH-Im-Bn-Br, and (*R,S*)-*cis*-Cy5-OH-Im-B-Br] to the neighboring OR group. In some cases, the favored dispositions obtained by theoretical calculations (see entries 2 and 4 in Table 4) are in good agreement with those observed experimentally in the solid state (see X-ray section below). In contrast, both *syn* (for bromide) and *anti* (for chloride) dispositions were found in the solid state for the *trans* six-membered ring (see below).<sup>[16]</sup> Interestingly, our theoretical model predicts a

small interaction energy difference (see entries 5 and 7 in Table 4) between the *syn* and *anti* conformers. This agreement represents a good validation of our theoretical model.

The theoretical calculations also reflect the differences between *cis* and *trans* isomers obtained experimentally from the melting data. Thus, these calculations consistently provide larger interaction energies for the *trans* isomers (compare entries 1 vs. 2 and 4 vs. 5 in Table 4). A closer inspection of the absolute values of the energies for the corresponding optimized structures (Supporting Information) shows that these differences are due to the higher stability of the isolated cations for the *cis* compounds. This extra stabilization could be due to a C2-H...OH hydrogen-bonding interaction, which seems to be more favorable for the *cis* isomers. However, the differences in  $T_m$  between cyclohexane and cyclopentane derivatives are not reflected in the computed interaction energy. This observation implies that these differences are more likely due to lattice packing effects rather than an effect of the intrinsic cation-anion interaction. The volume of the cation with a C6 cycle is slightly bigger than that with a C5 cycle. However, the latter has a larger conformational freedom, which may well contribute to increasing the number of possible conformations with an effect on the melting point.

The spectroscopic data also confirmed the differences observed between the *cis* and *trans* stereoisomers. Hydrogen-bonding effects in ionic liquids can be studied experimentally by techniques such as IR<sup>[23]</sup> or NMR<sup>[24]</sup> spectroscopy. In this case, the NMR spectra showed that the C2-H proton in *trans* derivatives resonates at lower field than that in the *cis* isomers [ $\delta = 10.13$  vs. 9.88 ppm for (*S,S*)-*trans*-Cy5-OH-Im-Bn-Br and (*R,S*)-*cis*-Cy5-OH-Im-Bn-Br, respectively, and  $\delta = 9.93$  vs. 9.75 ppm for (*S,S*)-*trans*-Cy6-OH-Im-Me-Br and (*R,S*)-*cis*-Cy6-OH-Im-Me-Br, respectively], thereby suggesting a weaker interaction between this proton and the anion in the *cis* diastereomers.<sup>[25]</sup> ATR-FTIR spectroscopy can also be used to study the interactions present in the *cis/trans* stereoisomers. NMR spectroscopy provides an average chemical shift for C2-H, C4-H, and C5-H interacting with the anion, whereas ATR-FTIR gives separate vibrational bands for distinct species, such as ion pairs, due to the different time scales of these techniques. In this case, the bands between 3300 and 3000  $\text{cm}^{-1}$  are considered diag-

nostic of the aromatic C-H bonds of the cations.<sup>[24,25]</sup> Vibrational bands at higher wavenumbers in this region correspond to C4-H and C5-H stretching modes whereas those at lower wavenumbers can be assigned to C2-H stretching modes.<sup>[26]</sup> The spectra of Cy6-Im-Bn-Br, a reference compound with no OR groups (Figure 3a), shows broad bands in this region. In the deconvoluted spectrum, the bands for C4-H, C5-H, and C2-H stretching modes are found at 3123, 3059, and 3028  $\text{cm}^{-1}$ , respectively, although these bands are clearly differentiated for the *cis* and *trans* imidazolium salts (Figure 3b and 3c). It is noteworthy that the bands at around 3170  $\text{cm}^{-1}$ , which are characteristic for the symmetric stretching vibration modes of the HC(4)-C(5)H moiety and are usually of weak intensity, are present in these spectra, thus indicating a stronger interaction between the anion and the cation, particularly for the *trans* diastereoisomer. The spectra also show a band corresponding to the C2-H stretching vibration with a lower vibrational frequency and higher intensity [peaks at 3090  $\text{cm}^{-1}$  for the C(2)-H moiety of (*R,S*)-*cis*-Cy6-OH-Im-Bn-Br and 3061  $\text{cm}^{-1}$  for (*S,S*)-*trans*-Cy6-OH-Im-Bn-Br]. This also suggests a stronger C2-H...X hydrogen bond and is in good agreement with the data obtained by using other experimental techniques.<sup>[27]</sup> The C2-H bond is weakened upon formation of a C2-H...X hydrogen bond therefore the frequency of its stretching vibration decreases. Such a decrease is usually accompanied by an increase in intensity and broadening of the band.<sup>[28]</sup>

The same tendency is also observed when liquid *cis/trans* diastereoisomeric imidazolium salt derivatives are compared

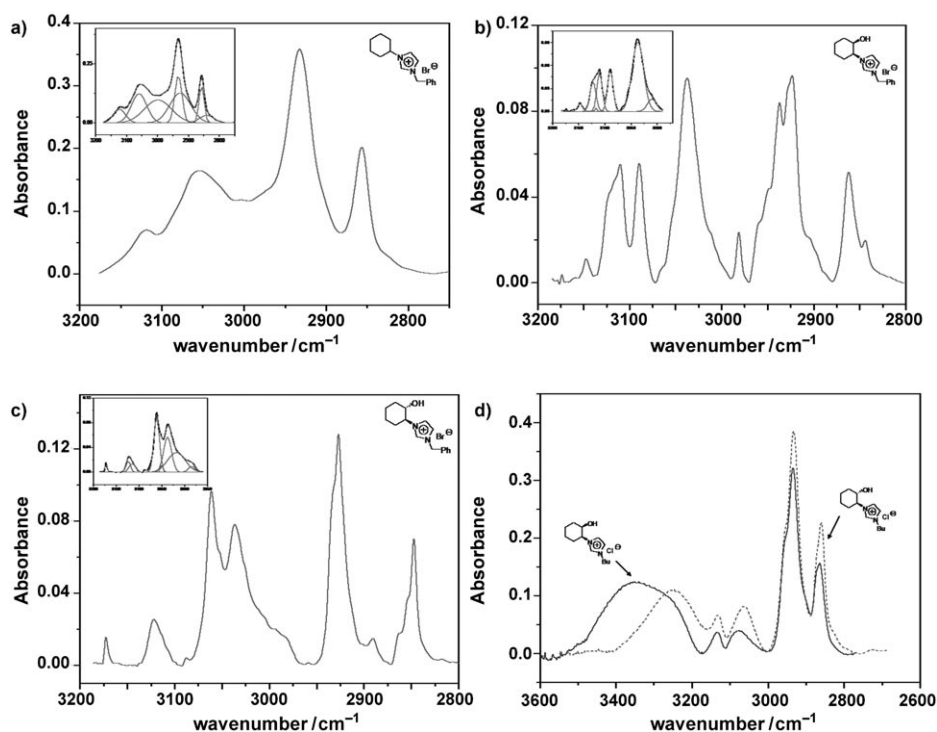


Figure 3. ATR-IR spectra for the CH stretching region. Insets show the deconvoluted infrared spectra: a) Cy6-Im-Bn-Br; b) (*R,S*)-*cis*-Cy6-OH-Im-Bn-Br; c) (*S,S*)-*trans*-Cy6-OH-Im-Bn-Br; d) (*R,S*)-*cis*-Cy6-OH-Im-Bu-Cl (line) and (*S,S*)-*trans*-Cy6-OH-Im-Bu-Cl (dashed line).

(see Figure 3d). For example, the spectrum of (*S,S*)-*trans*-Cy6-OH-Im-Bu-Cl shows stronger peaks corresponding to the C–H vibrational modes with an overall red shift when compared to those of the *cis* diastereoisomer. All these data suggest a more efficient interaction between the anion and the cation for the *trans* isomer.<sup>[29]</sup>

**Solid-state structures—X-ray diffraction analysis:** In order to better understand the differences observed for these chiral imidazolium salts, their intimate microscopic interactions should be studied at the molecular level. In this regard, we were able to grow crystals of several imidazolium salts suitable for X-ray diffraction analysis (Figure 4). Fortu-

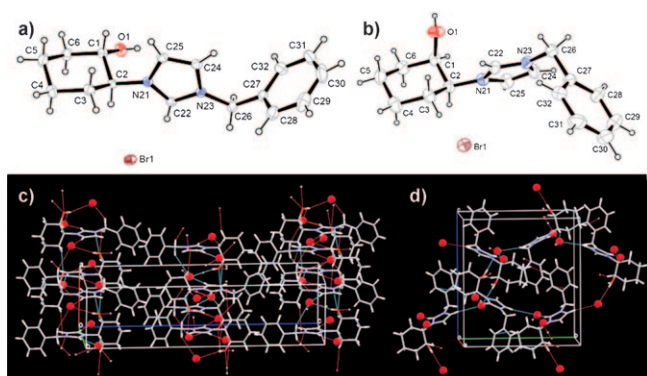


Figure 4. X-ray diffraction studies for a) (*S,S*)-*trans*-Cy6-OH-Im-Bn-Br; b) (*R,S*)-*cis*-Cy6-OH-Im-Bn-Br; c) crystal packing of (*S,S*)-*trans*-Cy6-OH-Im-Bn-Br; d) crystal packing of (*R,S*)-*cis*-Cy6-OH-Im-Bn-Br.

nately, the effect of the *cis/trans* relative configurations of the chiral centers could be systematically studied as we obtained crystals for both *cis*- and *trans*-Cy6-OH-Im-Bn-Br (Figure 4).<sup>[30]</sup> All the crystal structures showed short contacts between the anion and different hydrogen atoms of the chiral cation (See X-ray figure in the Supporting Information).<sup>[16]</sup> Both the hydroxyl and imidazolium moieties are involved in hydrogen bonding with the anion (either chloride or bromide), with those hydrogen bonds involving the imidazolium C2-H (C22-H in the crystal structure, Figure 4) moiety being especially noteworthy.<sup>[27]</sup> If we evaluate the hydrogen-bonding ability on the basis of the donor–acceptor distances a general trend can be seen for different X-H donors. Thus, the hydrogen-bonding distances increase in the sequence O–H < C22–H < C24–H/C25–H < C2–H < C26–H. However, it should be noted that the OH and imidazolium C2–H groups from a given cation are bound to different anions within the crystal lattice (see Figure 4c and 4d).

A more careful study of the crystal packing in the *cis* and *trans* forms of the cyclohexane derivatives [(*S,S*)-*trans*-Cy6-OH-Im-Bn-Br; and (*R,S*)-*cis*-Cy6-OH-Im-Bn-Br] showed a lower crystal density (1.3369 vs. 1.4128 g cm<sup>−3</sup>), larger cell volume (1675.3 vs. 1585.3 Å<sup>3</sup>), a lower number of intermolecular interactions per molecule (13 vs. 14), and a longer mean distance for the intermolecular contacts (2.826 vs.

2.715 Å) for the *cis* isomer.<sup>[16,31]</sup> In principle, this would mean a less compact lattice for the *cis* than for the *trans* diastereomer. Such differences can be correlated with the decrease in *T<sub>m</sub>* found for *cis* derivatives [Figure 2; *T<sub>m</sub>* = 188 vs. 156 °C for (*S,S*)-*trans*-Cy6-OH-Im-Bn-Br and (*R,S*)-*cis*-Cy6-OH-Im-Bn-Br, respectively].

We also analyzed the differences between the *cis/trans* relative configurations by means of a topological analysis of the Laplacian of the electron density as obtained from Fourier maps.<sup>[32]</sup> This analysis provided us with more unambiguous and incisive information regarding bonding interactions than that obtainable from comparing interatomic distances and allowed us to observe bonding beyond mere geometry. This analysis also provided valuable information about the topological magnitudes, which gives a rather accurate picture of the bonding. In (*R,S*)-*cis*-Cy6-OH-Bn-Br, for example, the O atom in the OH group exhibits two large non-bonding charge concentrations ( $\nabla^2\rho = -9.8$  and  $-10.0$  e Å<sup>−5</sup>), which correspond to lone pairs, and two smaller bonded charge concentrations ( $\nabla^2\rho = -5.1$  and  $-4.8$  e Å<sup>−5</sup>), which correspond to the C1–O1 and O1–H11 interactions, whereas the O atoms in the OH group of (*S,S*)-*trans*-Cy6-OH-Bn-Br exhibit three such maxima ( $\nabla^2\rho = -4.8$ ,  $-4.7$  and  $-10.1$  e Å<sup>−5</sup>) for the C1–O1 and O1–H11 interactions and one lone pair, respectively. However, an additional maximum of smaller magnitude ( $\nabla^2\rho = -7.3$  e Å<sup>−5</sup>), which indicates an additional noncovalently bonded charge concentration between the electron pairs of O11 and H22 of adjacent molecules, is also observed. The *trans* isomer therefore shows an additional interaction compared to the *cis* compound involving OH and C2–H (C-22 in the crystal structure) at the imidazolium ring.

Overall, the structural data obtained by X-ray diffraction, NMR and ATR-FTIR spectroscopy, and theoretical calculations suggest stronger cation–anion interactions for the *trans* isomers than for the *cis* ones, which nicely correlates with the observed physical (*T<sub>m</sub>*) properties of the ionic liquids. Moreover, our structural study located these distinguishing interactions at the OH group and the C2–H moiety of the imidazolium ring. Apart from anion–cation interactions, the topological analysis of experimental electron densities, as reconstructed from X-ray diffraction data for diastereomeric crystals, has allowed us to locate a noncovalent cation–cation bonding which must also have an important influence on the macroscopic properties.

**Racemic versus enantiopure chiral imidazolium salts:** We have demonstrated the key role played by the relative configuration of the chiral centers in the non-covalent interactions at the molecular level and, ultimately, in the physical properties of the CILs. In order to further confirm the importance of chirality, we also measured the melting temperatures of the corresponding racemic mixtures of the salts and found significant differences between the racemic and enantiopure compounds (see Table 5). Thus, with the exception of *trans*-Cy6-OH-Im-Bn-Br, the melting points of the racemic mixtures were found to be higher than those of the

Table 5. Effect of the enantiopurity on the melting points ( $T_m$ ) for some *cis*- and *trans*-imidazolium salts.

Imidazolium salt	$T_m$ [°C] <sup>[a]</sup> (enantiopure)	$T_m$ [°C] <sup>[a]</sup> (racemic mixture)
<i>trans</i> -Cy6-OH-Im-Bn-Br	188 ( <i>S,S</i> )	181 ( $\pm$ )
<i>cis</i> -Cy6-OH-Im-Bn-Br	156 ( <i>R,S</i> )	166 ( $\pm$ )
<i>trans</i> -Cy5-OH-Im-Bn-Br	112 ( <i>S,S</i> )	168 ( $\pm$ )
<i>cis</i> -Cy5-OH-Im-Bn-Br	19 ( <i>R,S</i> )	300 ( $\pm$ )

[a] Melting temperatures for a heating rate of 5°Cmin<sup>-1</sup> calculated at onset.

enantiomerically pure forms. This observation suggested that CILs tend to interact to form stable racemic conglomerates.

Fortunately, we also obtained experimentally conclusive data to support this assumption at the molecular level as we were able to grow crystals of a chiral imidazolium salt in both its enantiopure [(*S,S*)-*trans*-Cy5-OH-Im-Bn-Br, Figure 5a] and racemic [( $\pm$ )-*trans*-Cy5-OH-Im-Bn-Br, Fig-

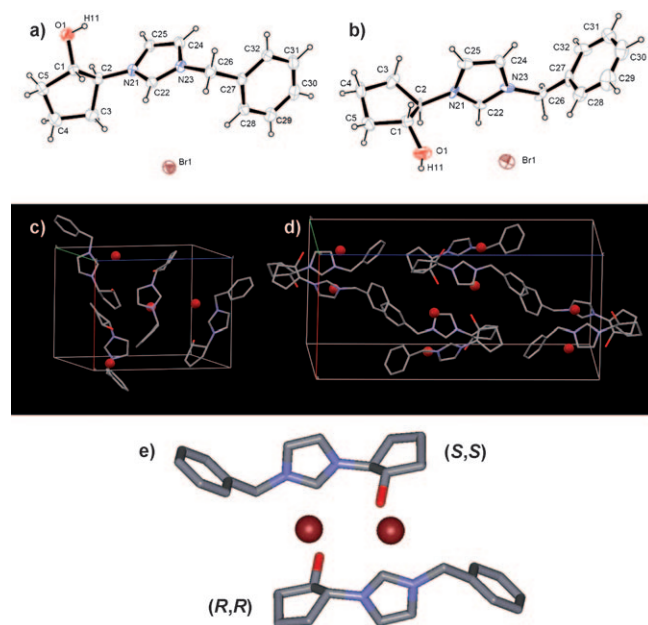


Figure 5. X-ray analysis and corresponding crystal packing of enantiopure (*S,S*)-*trans*-Cy5-OH-Im-Bn-Br (a and c) and racemic ( $\pm$ )-*trans*-Cy5-OH-Im-Bn-Br (b and d). An expansion of the heterochiral dimer observed in the crystal of the racemic form is shown in e).

ure 5b] forms suitable for X-ray analysis. The racemic salt is more tightly packed than the enantiopure one, as indicated by their different crystal densities (1.4203 and 1.4127 g cm<sup>-3</sup>, respectively). Furthermore, the disposition of the imidazolium ring with respect to the OH group is *syn* in the racemic compound (Figure 5b), which contrasts with the configuration obtained for the enantiopure crystal (Figure 5a) and that obtained from theoretical calculations on isolated ion pairs (Table 4). This conformational change must be produced by additional cation–cation interactions within the racemic compound. The topological analysis also produced

significant differences. Thus, the oxygen atom in the OH moiety of enantiopure (*S,S*)-*trans*-Cy5-OH-Im-Bn-Br exhibits two large nonbonded charge concentrations ( $\nabla^2\rho = -10.1$  and  $-10.3$  e Å<sup>-5</sup>), which correspond to lone pairs, and two smaller bonded charge concentrations ( $\nabla^2\rho = -5.3$  and  $-5.1$  e Å<sup>-5</sup>), which correspond to C1–O1 and O1–H11 interactions. In the racemic compound [( $\pm$ )-*trans*-Cy5-OH-Im-Bn-Br], in contrast, the O atoms in the OH moiety exhibit three such maxima ( $\nabla^2\rho = -5.2$ ,  $-5.1$ , and  $-10.3$  e Å<sup>-5</sup>) for the C1–O1 and O1–H11 interactions and one lone pair, respectively. However, a maxima of lower magnitude ( $\nabla^2\rho = -7.1$  e Å<sup>-5</sup>), which suggests an additional noncovalently bonded charge concentration between the electron pairs of O11 and H22 of adjacent molecules within the racemic crystal, is also observed. We therefore expanded the racemic crystal structure through the contacts corresponding to this additional interaction and obtained a heterochiral (racemic) non-covalent dimer connected through O1 and H22 of the imidazolium moiety and interrelated by a center of symmetry (one molecule with an *R,R* and the other with an *S,S* relative configuration; see Figure 5e). These data strongly support our initial hypothesis and correlate nicely with the melting values, thus highlighting the strong impact of chirality on the physical properties of imidazolium salts.

Both the racemic and enantiopure salts were also studied by ATR-FTIR spectroscopy. In general, the absorptions for the vibrational modes of OH and imidazolium C–H aromatic groups in the racemic salts appear at lower frequency, but are of higher intensity than those for the enantiopure form (Figure 6). It should be noted that the different trend in melting points observed for (*S,S*)-*trans*-Cy6-OH-Im-Bn-Br and the racemic mixture is also reflected in the C–H vibration modes of their imidazolium rings, with the peaks corresponding to these stretching modes being slightly red-shifted compared to those in the spectra of the racemic mixture. Thus, there is once again a perfect correlation between the binding interactions obtained from the topological analysis and the “classical” hydrogen-bonding interaction characterized by FT-IR spectroscopy, which ultimately allows us to explain the observed differences in physical macroscopic properties ( $T_m$ ).

## Conclusions

We have reported the chemoenzymatic modular synthesis and physical/structural study of a new family of more than 30 enantiopure imidazolium salts. This has allowed us to systematically map all the possible structural variables within the chiral molecules. The melting temperatures of these compounds have been found to differ significantly. Some of these variables (alkylating group or nature of the anion) were found to have similar effects to those reported previously for imidazolium-based ILs. Other structural vectors, such as cycloalkane ring size, the presence of polar groups in the cation structure and, especially, the configurations of the chiral centers have also been systematically studied. In

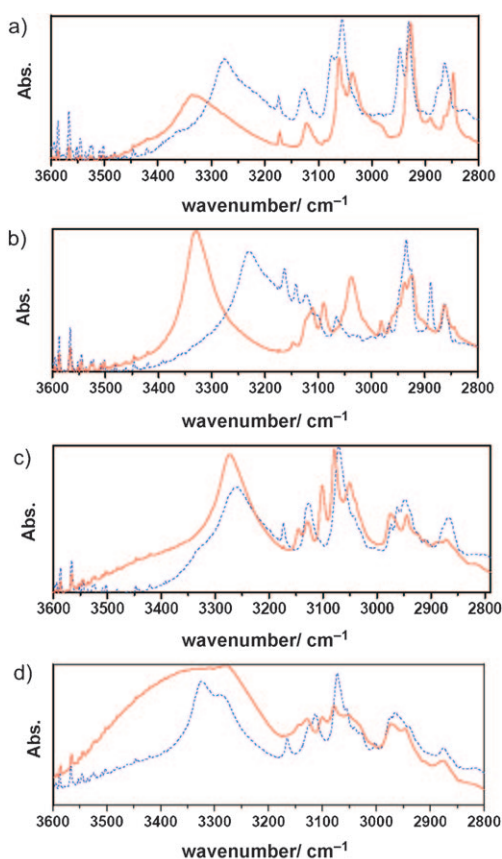


Figure 6. ATR-FT-IR spectra for enantiopure (red lines) and racemic mixtures (blue dashed lines) of: a) (*S,S*)-*trans*-Cy6-OH-Im-Bn-Br; b) (*R,S*)-*cis*-Cy6-OH-Im-Bn-Br; c) (*S,S*)-*trans*-Cy5-OH-Im-Bn-Br; d) (*R,S*)-*cis*-Cy5-OH-Im-Bn-Br.

general, five-membered rings lead to salts with lower melting temperatures than six-membered rings, probably due to a different degree of conformational freedom. The presence of hydrogen-bonding groups also increases the  $T_m$  of the imidazolium salts. Finally, a *trans* configuration also increases  $T_m$  with respect to the *cis* isomers. A multidisciplinary approach involving spectroscopic (NMR, FT-IR-ATR) and theoretical studies has shown that the observed differences mainly arise from the anion–cation interactions. Thus, we obtained a reasonable correlation between the observed melting points and the theoretical anion–cation interaction energies for model compounds. Furthermore, the spectroscopic data reflect the key role played by hydrogen bonds between the OH and imidazolium C2H moieties, and an X-ray diffraction study (including topological analysis of *cis/trans* isomers) of several compounds allowed us to locate additional inter-cation interactions involving these groups. These interactions are a major cause of the differences in properties of stereoisomeric salts.

Even more interestingly, we also studied the effect of chirality by comparing enantiopure CILs with their racemic mixtures. The surprising differences observed can also be explained by the corresponding spectroscopic and crystallographic data and are also intimately related with interac-

tions between the OH group and the imidazolium ring. Thus, in one case we observed the formation of heterochiral (racemic) conglomerates through non-covalent interactions between OH and C2-H, which increases the melting temperature of the racemates.

Overall, we have been able to prepare and characterize a broad family of new enantiopure CILs by systematic structural modifications. Moreover, the differences in macroscopic properties ( $T_m$ ) have been successfully correlated with non-covalent interactions observed by microscopic structural data from experimental (NMR, FT-IR-ATR, X-ray) and theoretical studies. We expect that these findings will help us to better understand the properties of these neoteric solvents, especially the effect of chirality. A full understanding will allow an improved bottom-up design and lead to the preparation of new CILs with preselected properties.

Our study demonstrates that chirality has significant impact on the physical properties of imidazolium salts. The relative configuration of the chiral centers and the presence of both enantiomers within the mixture also significantly affects the macroscopic properties. These results show that compounds with a similar structure do not necessarily have similar interactions.

## Experimental Section

**Materials:** *Candida antarctica* lipase type B (CAL-B, Novozyme 435, 7300 PLU/g) was a gift from Novozymes. *Pseudomonas cepacia* lipase PSL-C II (1019 U/g) and PSL-C I (1638 U/g) were purchased from Amano Pharmaceutical Co. and Sigma–Aldrich respectively. Porcine pancreas lipase (PPL, 46 U/mg) and *Candida cylindracea* lipase (CRL, 1141 U/mg) were purchased from Sigma. *Candida antarctica* lipase type A [Chirazyme L-5, c-f, lyophilized, (1000 U/g using tributyrin)] was purchased from Roche. All other reagents were purchased from different commercial sources and used without further purification. Solvents were distilled over an appropriate desiccant under nitrogen. Flash chromatography was performed on silica gel 60 (230–240 mesh).  $^1\text{H}$ ,  $^{13}\text{C}$ , DEPT, and  $^1\text{H}$ - $^{13}\text{C}$  heteronuclear NMR experiments were performed on AV-300 ( $^1\text{H}$ : 300.13 MHz;  $^{13}\text{C}$ : 75.5 MHz), DPX 300 ( $^1\text{H}$ : 300.13 MHz;  $^{13}\text{C}$ : 75.5 MHz), AV-400 ( $^1\text{H}$ : 400.13 MHz;  $^{13}\text{C}$ : 100.6 MHz), or AV-600 ( $^1\text{H}$ : 600.13 MHz) spectrometers. Chemical shifts are given in delta ( $\delta$ ) units and the coupling constants ( $J$ ) in hertz (Hz). ESI $^+$  or APCI $^+$  mass spectra were recorded with an HP1100 chromatograph mass spectrometer. Microanalyses were performed using a Perkin–Elmer model 2400 instrument. Optical rotations were measured with a Perkin–Elmer 241 polarimeter. High performance liquid chromatography (HPLC) analyses were completed by using a Hewlett Packard 1100 chromatograph UV detector at 210 nm using a Daicel CHIRALCEL OD, CHIRALCEL OB-H, or a CHIRAL-PAK AS column (25 cm  $\times$  4.6 mm I.D.). Further detailed data are provided in the Supporting Information.

General procedures for substrate synthesis

( $\pm$ )-*trans*-**3a**: Cyclopentene oxide (3.18 mL, 36.72 mmol) was added to a solution of imidazole (2.00 g, 29.38 mmol) in 1,4-dioxane (16 mL) and the solution stirred for 18 h at 100 °C. The solvent was then evaporated under reduced pressure and the resulting crude mixture purified by flash chromatography (10% MeOH/ $\text{CHCl}_3$ ) to give 3.92 g of ( $\pm$ )-*trans*-**3a** as a white solid (88% yield).

( $\pm$ )-*trans*-**4a**:  $\text{Et}_3\text{N}$  (277  $\mu\text{L}$ , 1.97 mmol), DMAP (27 mg, 0.22 mmol), and  $\text{Ac}_2\text{O}$  (123  $\mu\text{L}$ , 1.31 mmol) were added successively to a solution of ( $\pm$ )-*trans*-**3a** (100 mg, 0.66 mmol) in dry  $\text{CH}_2\text{Cl}_2$  (10 mL) under nitrogen. The mixture was stirred at room temperature for 4 h until complete consump-

tion of the starting material, then the solvent was evaporated under reduced pressure. The crude reaction mixture was then purified by flash chromatography on silica gel (5% MeOH/CHCl<sub>3</sub>) to give 125 mg of ( $\pm$ )-*trans*-4a as a pale-yellow oil (97% yield).

**Enzymatic kinetic resolution of racemic *cis*- and *trans*-alcohols 3a–b:** Vinyl acetate (1.64 mL, 17.82 mmol) was added to a suspension of the racemic alcohol (5.94 mmol) and the corresponding enzyme (1:1 weight ratio with respect to the alcohol) in dry THF (59 mL) under nitrogen and the mixture shaken, depending on the substrate, at between 30 and 60°C at 250 rpm. Aliquots were regularly analyzed by HPLC until 50% conversion, then the reaction was quenched and the enzyme filtered and washed with CH<sub>2</sub>Cl<sub>2</sub> (3 × 50 mL). The solvent was evaporated under reduced pressure and the crude reaction mixture purified by flash chromatography on silica gel (5–10% MeOH/CHCl<sub>3</sub>) to afford the corresponding optically enriched acetate and alcohol (see Tables 1 and 2).

**Mitsunobu reaction:** The corresponding acid (4.32 mmol), PPh<sub>3</sub> (1.36 g, 5.18 mmol), and DEAD (0.82 mL, 5.18 mmol) were successively added to a solution of the corresponding *trans*-alcohol 3a–b (4.32 mmol) in dry THF (22 mL) under nitrogen. The mixture was stirred for 2 h until starting material could no longer be detected by TLC analysis. The organic solvent was evaporated under reduced pressure and the crude mixture used directly for the deprotection step.

**Deprotection step:** K<sub>2</sub>CO<sub>3</sub> (595 mg, 4.32 mmol) and H<sub>2</sub>O (6.8 mL) were added to a solution of the crude product from the Mitsunobu reaction in MeOH (6.8 mL). This mixture was stirred for 1 h and then the MeOH was evaporated under reduced pressure. The resulting suspension was redissolved in H<sub>2</sub>O (10 mL), a solution of brine was added (5 mL), and the mixture extracted with EtOAc (3 × 10 mL). The corresponding *cis*-alcohol was isolated as a white solid (78–85% overall yield for both steps) by flash chromatography on silica gel (5–10% MeOH/CH<sub>2</sub>Cl<sub>2</sub>).

Reaction between imidazole derivatives and benzyl bromide

a) *trans*-derivatives: A mixture of the alcohol (3 mmol) and benzyl bromide (3.62 mmol) in MeCN (2.3 mL) was stirred for 2.5 h at 70°C, then the reaction was cooled to room temperature and the resulting gummy product washed with Et<sub>2</sub>O (5 × 10 mL) to afford the corresponding bromide salt as a white solid (93–96% yield).

b) *cis*-derivatives: A mixture of the alcohol (3 mmol) and benzyl bromide (60 mmol) was stirred for 2.5 h at 70°C, then the reaction was cooled to room temperature and the resulting gummy product washed with Et<sub>2</sub>O (5 × 10 mL) to afford the corresponding bromide salt as a white solid (96–97% yield).

**Anion-exchange reaction with LiNTf<sub>2</sub>:** A solution of lithium bis(trifluoromethane) sulfonimide (467 mg, 1.63 mmol) in H<sub>2</sub>O (1.5 mL) was added to a solution of the corresponding bromide or chloride salt (1.48 mmol) in MeOH (40 mL), and the resulting mixture stirred for the required time at room temperature (see Table 3). MeOH was then evaporated at reduced pressure, further H<sub>2</sub>O (20 mL) added, and the mixture extracted with CH<sub>2</sub>Cl<sub>2</sub> (3 × 20 mL). The organic phases were combined, dried over Na<sub>2</sub>SO<sub>4</sub>, and the solvent evaporated under reduced pressure to afford the corresponding imidazole salt as a light yellowish liquid (78–97% yield).

**Anion-exchange reaction with NaBF<sub>4</sub>:** A solution of sodium tetrafluoroborate (92 mg, 0.84 mmol) in H<sub>2</sub>O (580  $\mu$ L) was added to a solution of the corresponding bromide or chloride salt (0.56 mmol) in MeOH (14.4 mL) and the resulting mixture stirred for 90 h at room temperature. The solvent was then evaporated under reduced pressure and the resulting solid residue washed with CH<sub>2</sub>Cl<sub>2</sub> (3 × 8 mL). The insoluble salts were filtered off and the solvent evaporated under reduced pressure to afford the corresponding imidazole salt as a light yellowish liquid (85–94% yield).

**Differential scanning calorimetry:** Glass-transition temperatures and melting points were measured by using a Mettler–Toledo differential scanning calorimeter (DSC), model DSC822e. The instrument was calibrated for temperature and heat flow with zinc and indium reference samples provided by Mettler–Toledo. Samples were placed in a 40-mL, hermetically sealed aluminum pan with a pinhole in the top. An empty aluminum pan was used as the reference. Samples were exposed to a flowing N<sub>2</sub> atmosphere. Before the DSC test, each sample was dried at

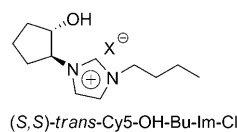
90–100°C and 10<sup>-2</sup>–10<sup>-3</sup> mbar for 4 h, and was further dried in situ in the differential scanning calorimeter by holding the sample at 130°C for 120 min as the presence of volatiles, especially water, can affect the glass-transition and melting temperatures. Melting transition temperatures were determined by multiple cycles (typically three) involving heating the sample from –65 to 250°C, followed by cooling from 250 to –65°C, both at a rate of 5°C min<sup>-1</sup>. The melting temperatures were determined at the onset of the transition.

## Acknowledgements

Financial support from the Ministerio de Ciencia e Innovación (MICINN CTQ2007-61126, CTQ2008-04415, and CTQ2008-04309), CSIC-I3 (2007801001), and BANCAIXA (P1 1A2007-11) is gratefully acknowledged. V.G.-F and E.G.-V. (Ramón y Cajal Program), and R.P. (FPU) thank the MICINN for personal funding. N.R.-L. thanks the FICYT for a pre-doctoral fellowship.

- a) S. Z. E. Abedin, F. Endres, *Acc. Chem. Res.* **2007**, *40*, 1106–1113; b) R. D. Rogers, G. A. Voth, *Acc. Chem. Res.* **2007**, *40*, 1077–1078; c) R. D. Rogers, K. R. Seddon, *Ionic Liquids III: Fundamentals, Progress, Challenges, and Opportunities*, ACS, Washington, **2005**; d) P. Wasserscheid, T. Welton, *Ionic Liquids in Synthesis*, Wiley-VCH, Weinheim, **2007**.
- a) N. V. Plechkova, K. R. Seddon, P. Tundo, A. Perosa, F. Zecchini, *Methods and Reagents for Green Chemistry*, Wiley, New York, **2007**, pp. 103–130; b) R. D. Rogers, K. R. Seddon, *Ionic Liquids as Green Solvents, Progress and Prospects*, ACS, Washington, **2003**; c) R. D. Rogers, K. R. Seddon, S. Volkov, *Green Industrial Applications of Ionic Liquids*, Kluwer Academic, Norwell, **2003**; d) R. D. Rogers, K. R. Seddon, *Ionic Liquids: Industrial Applications for Green Chemistry*, ACS, Washington **2002**; e) M. J. Earle, K. R. Seddon, *Pure Appl. Chem.* **2000**, *72*, 1391–1398.
- a) Š. Toma, M. Mečiarová, R. Šebesta, *Eur. J. Org. Chem.* **2009**, 321–327; b) N. V. Plechkova, K. R. Seddon, *Chem. Soc. Rev.* **2008**, *37*, 123–150; c) S. Chowdhury, R. S. Mohan, J. L. Scott, *Tetrahedron* **2007**, *63*, 2363–2389; d) N. Jain, A. Kumar, S. Chauhan, S. M. S. Chauhan, *Tetrahedron* **2005**, *61*, 1015–1060; e) T. Welton, *Coord. Chem. Rev.* **2004**, *248*, 2459–2477; f) P. Wasserscheid, W. Keim, *Angew. Chem.* **2000**, *112*, 3926–3945; *Angew. Chem. Int. Ed.* **2000**, *39*, 3772–3789; g) T. Welton, *Chem. Rev.* **1999**, *99*, 2071–2083.
- a) X. Han, D. W. Armstrong, *Acc. Chem. Res.* **2007**, *40*, 1079–1086; b) S. T. Anjan, *Chem. Eng. Prog.* **2006**, *102*, 30–39; c) H. Zhao, S. Xiao, P. Ma, *J. Chem. Technol. Biotechnol.* **2005**, *80*, 1089–1096; d) A. E. Visser, R. P. Swatoski, W. M. Reichert, R. Mayton, S. Sheff, A. Wierzbicki, J. H. Davis, R. D. Rogers, *Environ. Sci. Technol.* **2002**, *36*, 2523–2529; e) J. G. Huddleston, R. D. Rogers, *Chem. Commun.* **1998**, 1765–1766.
- D. MacFarlane, M. Forsyth, *The Handbook of Ionic Liquids: Electrochemistry*, Wiley-VCH, Weinheim, **2008**.
- a) H. Weingärtner, *Angew. Chem.* **2008**, *120*, 664–682; *Angew. Chem. Int. Ed.* **2008**, *47*, 654–670; b) H. Tokuda, K. Ishii, M. A. B. H. Susan, S. Tsuzuki, K. Hayamizu, M. Watanabe, *J. Phys. Chem. B* **2006**, *110*, 2833–2839; c) H. Tokuda, K. Hayamizu, K. Ishii, M. A. B. H. Susan, M. Watanabe, *J. Phys. Chem. B* **2005**, *109*, 6103–6110; d) Z.-B. Zhou, H. Matsumoto, K. Tatsumi, *Chem. Eur. J.* **2004**, *10*, 6581–6591; e) H. Tokuda, K. Hayamizu, K. Ishii, M. A. B. H. Susan, M. Watanabe, *J. Phys. Chem. B* **2004**, *108*, 16593–16600; f) J. G. Huddleston, A. E. Visser, W. M. Reichert, H. D. Willauer, G. A. Broker, R. D. Rogers, *Green Chem.* **2001**, *3*, 156–164; g) J. D. Holbrey, K. R. Seddon, *J. Chem. Soc. Dalton Trans.* **1999**, 2133–2140.
- a) W. L. Hough-Troutman, M. Smiglak, S. Griffin, W. M. Reichert, I. Mirska, J. Jodynis-Liebert, T. Adamska, J. Nawrot, M. Stasiewicz, R. D. Rogers, J. Pernak, *New J. Chem.* **2009**, *33*, 26–33; b) M. Smi-

- glak, A. Metlen, R. D. Rogers, *Acc. Chem. Res.* **2007**, *40*, 1182–1192.
- [8] a) K. E. Gutowski, E. J. Maginn, *J. Am. Chem. Soc.* **2008**, *130*, 14690–14704; b) M. D. Soutullo, C. I. Odom, B. F. Wicker, C. N. Henderson, A. C. Stenson, J. H. Davis, Jr., *Chem. Mater.* **2007**, *19*, 3581–3583; c) S. Lee, *Chem. Commun.* **2006**, 1049–1063; d) J. H. Davis, Jr., *Chem. Lett.* **2004**, *33*, 1072–1077.
- [9] For general reviews of chiral ionic liquids, see: a) K. Bica, P. Gaertner, *Eur. J. Org. Chem.* **2008**, 3235–3250; b) A. Winkel, P. V. G. Reddy, R. Wilhelm, *Synthesis* **2008**, 999–1016; c) X. Chen, X. Li, A. Hu, F. Wang, *Tetrahedron: Asymmetry* **2008**, *19*, 1–14; d) A. D. Headley, B. Ni, *Aldrichimica Acta* **2007**, *40*, 107–117; e) C. Baudequin, D. Brjgeon, J. Levillain, F. Guillen, J.-C. Plaquevent, A.-C. Gaumont, *Tetrahedron: Asymmetry* **2005**, *16*, 3921–3945; f) J. Ding, D. W. Armstrong, *Chirality* **2005**, *17*, 281–292; g) C. Baudequin, J. Baudoux, J. Levillain, D. Cahard, A.-C. Gaumont, J.-C. Plaquevent, *Tetrahedron: Asymmetry* **2003**, *14*, 3081–3093.
- [10] a) K. Schneiders, A. Bösmann, P. S. Schulz, P. Wasserscheid, *Adv. Synth. Catal.* **2009**, *351*, 432–440; b) D. Chen, M. Schmitkamp, G. Franciò, J. Klankermayer, W. Leitner, *Angew. Chem.* **2008**, *120*, 7449–7451; *Angew. Chem. Int. Ed.* **2008**, *47*, 7339–7341; c) T. Yu, T. Yamada, G. C. Gaviola, R. G. Weiss, *Chem. Mater.* **2008**, *20*, 5337–5344; d) T. Yamada, P. J. Lukac, T. Tao Yu, R. G. Weiss, *Chem. Mater.* **2007**, *19*, 4761–4768; e) B. Ni, A. D. Headley, *Tetrahedron Lett.* **2006**, *47*, 7331–7334; f) S. V. Malhotra, Y. Wang, *Tetrahedron: Asymmetry* **2006**, *17*, 1032–1035; g) C. Luys, L. C. Branco, P. M. P. Gois, N. M. T. Lourenço, V. B. Kurteva, C. A. M. Afonso, *Chem. Commun.* **2006**, 2371–2372; h) F. Guillen, D. Bregeond, J.-C. Plaquevent, *Tetrahedron Lett.* **2006**, *47*, 1245–1248; i) R. Gausepohl, P. Buskens, J. Kleinen, A. Bruckmann, C. W. Lehmann, J. Klankermayer, W. Leitner, *Angew. Chem.* **2006**, *118*, 3772–3775; *Angew. Chem. Int. Ed.* **2006**, *45*, 3689–3692.
- [11] a) J.-C. Plaquevent, J. Levillain, F. Guillen, C. Malhiac, A.-C. Gaumont, *Chem. Rev.* **2008**, *108*, 5035–5060; b) H. Ohno, K. Fukumoto, *Acc. Chem. Res.* **2007**, *40*, 1122–1129.
- [12] a) F. Neve, A. Crispini, *CrystEngComm* **2007**, *9*, 698–703; b) D. Zhao, Z. Fei, W. H. Ang, R. Scopelliti, P. J. Dyson, *Eur. J. Inorg. Chem.* **2007**, 279–284; c) N. K. Sharma, M. D. Tickell, J. L. Anderson, J. Kaar, V. Pino, B. F. Wicker, D. W. Armstrong, J. H. Davis, Jr., A. J. Russell, *Chem. Commun.* **2006**, 646–648; d) Z. Fei, T. J. Geldbach, D. Zhao, P. J. Dyson, *Chem. Eur. J.* **2006**, *12*, 2122–2130; e) J. Y. Z. Chiou, J. N. Chen, J. S. Lei, I. J. B. Lin, *J. Mater. Chem.* **2006**, *16*, 2972–2977; f) D. Zhao, Z. Fei, R. Scopelliti, P. J. Dyson, *Inorg. Chem.* **2004**, *43*, 2197–2205; g) L. C. Branco, J. N. Rosa, J. J. Moura Ramos, C. A. M. Afonso, *Chem. Eur. J.* **2002**, *8*, 3671–3677.
- [13] A. J. Bailey, C. Lee, R. K. Feller, J. B. Orton, C. Mellot-Draznieks, B. Slater, W. T. A. Harrison, P. Simoncic, A. Navrotsky, M. C. Groschel, A. K. Cheetham, *Angew. Chem.* **2008**, *120*, 8762–8765; *Angew. Chem. Int. Ed.* **2008**, *47*, 8634–8637.
- [14] I. Krossing, J. M. Slattery, C. Daguene, P. J. Dyson, A. Oleinikova, H. Weingärtner, *J. Am. Chem. Soc.* **2006**, *128*, 13427–13434.
- [15] R. Torregrosa, I. M. Pastor, M. Yus, *Tetrahedron* **2007**, *63*, 469–473.
- [16] Some preliminary synthetic results regarding the preparation of chiral imidazolium salts have been reported previously: E. Busto, N. Ríos-Lombardía, V. Gotor-Fernández, E. García-Verdugo, I. Alfonso, A. Menéndez-Velázquez, S. García-Granda, M. I. Burguete, S. V. Luis, V. Gotor, *Tetrahedron Lett.* **2007**, *48*, 5251–5254.
- [17] See the Supporting Information for additional data.
- [18] L. M. Levy, I. Lavandera, V. Gotor, *Org. Biomol. Chem.* **2004**, *2*, 2572–2577.
- [19] The nomenclature of imidazolium salts is defined by seven descriptors: The first one includes the absolute configuration of C1 and C2 at the cycloalkyl ring [for instance: (*S,S*)]. The relative configuration at these carbon atoms is reported by the second descriptor *trans* or *cis* [for instance: (*S,S*)-*trans*]. The size of the cycloalkyl ring is described through the use of the terms Cy5 for cyclopentane rings and Cy6 for cyclohexane rings [for instance: (*S,S*)-*trans*-Cy5]. The fourth descriptor indicates the presence of OH or OR at C2 of the cycloalkyl ring [for instance: (*S,S*)-*trans*-Cy5-OH-]. The nature of the alkyl chain at N3 of the imidazolium moiety is indicated by the use of Bn (for benzyl), Bu (for butyl), or Oct (for octyl) [for instance: (*S,S*)-*trans*-Cy5-OH-Bu-]. Finally, the term Im refers to the central core of imidazolium, while the last descriptor refers to the specific anion included in the structure [for instance: (*S,S*)-*trans*-Cy5-OH-Bu-Im-Cl].
- [20] See the Supporting Information for a complete list of yields and  $T_m$ 's for all the ionic liquids prepared in this work.
- [21] a) R. Ludwig, *Phys. Chem. Chem. Phys.* **2008**, *10*, 4333–4339; b) B. L. Bhargava, S. Balasubramanian, M. L. Klein, *Chem. Commun.* **2008**, 3339–3351; c) S. A. Katsyuba, E. E. Zvereva, A. Vidiš, P. J. Dyson, *J. Phys. Chem. A* **2007**, *111*, 352–370; d) H. Markusson, J. P. Belires, P. Johansson, C. A. Angell, P. Jacobsson, *J. Phys. Chem. A* **2007**, *111*, 8717–8723; e) P. A. Hunt, B. Kirchner, T. Welton, *Chem. Eur. J.* **2006**, *12*, 6762–6775; f) C. J. Margulis, *Mol. Phys.* **2004**, *102*, 829–838; g) A. T. Elizabeth, C. C. Pye, R. D. Singer, *J. Phys. Chem. A* **2003**, *107*, 2277–2288.
- [22] a) G. D. Smith, O. Borodin, L. Li, H. Kim, Q. Liu, J. E. Bara, D. L. Ginc, R. Nobel, *Phys. Chem. Chem. Phys.* **2008**, *10*, 6301–6312; b) Q. Zhang, Z. Li, J. Zhang, S. Zhang, L. Zhu, J. Yang, X. Zhang, Y. Deng, *J. Phys. Chem. B* **2007**, *111*, 2864–2872; c) Z. Fei, W. H. Ang, D. Zhao, R. Scopelliti, E. E. Zvereva, S. A. Katsyuba, P. J. Dyson, *J. Phys. Chem. B* **2007**, *111*, 10095–10108; d) J. Y. Z. Chiou, J. N. Chen, J. S. Lei, I. J. B. Lin, *J. Mater. Chem.* **2006**, *16*, 2972–2977.
- [23] a) O. Höfft, S. Bahr, V. Kempter, *Langmuir* **2008**, *24*, 11562–11566; b) K. Fumino, A. Wulf, R. Ludwig, *Angew. Chem.* **2008**, *120*, 3890–3894; *Angew. Chem. Int. Ed.* **2008**, *47*, 3830–3834; c) A. Yokozeki, D. J. Kasprzak, M. B. Shiflett, *Phys. Chem. Chem. Phys.* **2007**, *9*, 5018–5026; d) N. E. Heimer, R. E. Del Sesto, Z. Meng, J. S. Wilkes, W. R. Carper, *J. Mol. Liq.* **2006**, *124*, 84–95; e) S. A. Katsyuba, P. J. Dyson, E. E. Vandyukova, A. V. Chernova, A. Vidiš, *Helv. Chim. Acta* **2004**, *87*, 2556–2565.
- [24] a) R. C. Remsing, J. L. Wildin, A. L. Rapp, G. Moyna, *J. Phys. Chem. B* **2007**, *111*, 11619–11621; b) J. Palomar, V. R. Ferro, M. A. Gilarranz, J. J. Rodriguez, *J. Phys. Chem. B* **2007**, *111*, 168–180; c) S. H. Chung, R. Lopato, S. G. Greenbaum, H. Shirota, E. W. Castner, Jr., J. F. Wishart, *J. Phys. Chem. B* **2007**, *111*, 4885–4893; d) D. Bankmann, R. Giernoth, *Prog. Nucl. Magn. Reson. Spectrosc.* **2007**, *51*, 63–90; e) J.-F. Huang, P.-Y. Chen, I.-W. Sun, S. P. Wang, *Inorg. Chim. Acta* **2001**, *320*, 7–11.
- [25] T. Köddermann, C. Wertz, A. Heintz, R. Ludwig, *ChemPhysChem* **2006**, *7*, 1944–1949.
- [26] K. Fumino, A. Wulf, R. Ludwig, *Angew. Chem.* **2008**, *120*, 8859–8862; *Angew. Chem. Int. Ed.* **2008**, *47*, 8731–8734.
- [27] a) S. Zahn, F. Uhlig, J. Thar, C. Spickermann, B. Kirchner, *Angew. Chem.* **2008**, *120*, 3695–3697; *Angew. Chem. Int. Ed.* **2008**, *47*, 3639–3641; b) S. Tsuzuki, H. Hiroyuki Tokuda, M. Mikami, *Phys. Chem. Chem. Phys.* **2007**, *9*, 4780–4784; c) K. Dong, S. Zhang, D. Wang, X. Yao, *J. Phys. Chem. A* **2006**, *110*, 9775–9782.
- [28] A. V. Iogansen, *Spectrochim. Acta Part A* **1999**, *55*, 1585–1612.
- [29] The computed vibrational frequencies of the C2–H bond for the obtained minima showed similar trends to the experimental ones (see the Supporting Information). Thus, the *trans* isomers showed absorptions at lower frequencies than the *cis* ones, in good accordance with the experimental data and reflecting the somehow stronger anion–cation interaction in the *trans* diastereoisomer. Although the computed (uncorrected) quantitative values of vibrational frequencies are far from the experimental ones, we believe that the correlation is qualitatively acceptable considering the number of approximations made.
- [30] We also attempted to record circular dichroism spectra to further support these observations. Unfortunately, the very low UV absorption of the imidazolium group precluded suitable spectra from being obtained.



- [31] All these parameters were calculated with the Mercury 1.3.2 software, developed by The Cambridge Crystallographic Data Centre and freely downloadable at: [www.ccdc.cam.ac.uk/products/mercury/](http://www.ccdc.cam.ac.uk/products/mercury/).
- [32] a) R. F. W. Bader, *J. Phys. Chem. A* **2007**, *111*, 7966–7972; b) “The Lagrangian Approach to Chemistry”: R. F. W. Bader, C. F. Matta, R. Boyd, in *Quantum Theory of Atoms in Molecules: From Solid State to DNA and Drug Design*, Wiley-VCH, Weinheim, **2007**, pp. 37–59; c) A. Menéndez-Velázquez, S. García Granda, *J. Appl. Crystallogr.* **2003**, *36*, 193–205; d) R. F. W. Bader, *Chem. Rev.* **1991**, *91*, 893–928; e) R. F. W. Bader, *Atoms in Molecules—A Quantum Theory*, Oxford University Press, Oxford, **1990**; f) R. F. W. Bader, R. J. Gillespie, P. J. MacDougall, *J. Am. Chem. Soc.* **1988**, *110*, 7329–7336.

Received: June 14, 2009  
Published online: November 27, 2009